Parameterized Model Order Reduction for Efficient Time and Frequency Domain Global Sensitivity Analysis of PEEC Circuits

L. De Camillis [1], G. Antonini [1], and F. Ferranti [2]

[1]UAq EMC Laboratory, Dipartimento di Ingegneria Industriale e dell'Informazione e di Economia,
Università degli Studi dell'Aquila, Via G. Gronchi 18, 67100, L'Aquila, Italy
luca.decamillis@gmail.com, giulio.antonini@univaq.it

[2]Department of Fundamental Electricity and Instrumentation,
Vrije Universiteit Brussel, Pleinlaan 2, B-1050 Brussels, Belgium
francesco.ferranti@vub.ac.be

Abstract – This paper presents a new parameterized model order reduction technique to efficiently perform global time- and frequency-domain sensitivity analysis of electromagnetic systems over the design space of interest. The partial element equivalent circuit (PEEC) method is adopted to build the electromagnetic system model at a set of initial samples in the design space. The block Laguerre-SVD algorithm is proposed to reduce the size of the original equations of the PEEC-based equivalent circuit along with those describing the port voltage and current sensitivities. Then, a multivariate cubic spline interpolation method is used to build a parameterized compact model of port voltages and currents along with their corresponding sensitivities over the entire design space of interest. Finally, two numerical examples are presented, which confirm the accuracy and efficiency of the proposed method.

Index Terms – Parameterized model order reduction, partial element equivalent circuit, sensitivity analysis, time- and frequency-domain circuit simulation.

I. INTRODUCTION

The need to improve the performances of electromagnetic (EM) structures during their early design stage has made sensitivity analysis a necessary tool. The sensitivities represent the system response gradients in the design parameter space, where the design parameters are related to the geometry and/or the materials of the EM structure.

The simplest way to compute sensitivities is represented by the perturbation method, which requires to analyze the EM structure for two different values of each design parameter for a specific nominal point in the design space. It is computationally expensive and often inaccurate, therefore impractical when the number of design parameters to take into account is large and a global sensitivity analysis over the design space of interest is required. Recently, significant progress has been made towards the development of sensitivity analysis approaches to be used along with EM simulators, involving conducting and dielectric objects, both in time- and frequency-domain [1–8]. Differential and integral equation-based methods have been considered for sensitivity analysis [9, 10]. Typical fields of applications are optimization of microwave devices, modeling of signal integrity (SI)/power integrity (PI) problems, control of crosstalk for electromagnetic compatibility (EMC) purposes. These techniques usually turn to be highly demanding in terms of both CPU time and memory resources, since they perform the sensitivity analysis using EM solvers and/or manipulating matrices describing the EM system which are typically very large.

Among EM methods, the partial element equivalent circuit (PEEC) [11] has gained increasing popularity because of its ability to transform the EM system under examination into an equivalent circuit [11–16] that can be represented by modified nodal analysis (MNA) matrix circuit equations [17], studied by means of Kirchoff principles and simulated using circuit solvers. The PEEC method uses a circuit interpretation of the electric field integral equation (EFIE) [18].

In the context of sensitivity analysis, a PEEC-based method to carry out parameterized sensitivity analysis of EM systems that depend on multiple design parameters has been proposed in [19]. The PEEC method is used to compute state-space matrices of the MNA equations for a set of values of design parameters (e.g., geometrical and substrate parameters). An interpolation process provides parameter-

Submitted On: August 25, 2015
Accepted On: January 25, 2016

ized models of these matrices as functions of design parameters [20]. The proposed interpolation scheme is able to compute derivatives of EM matrices, which are needed to perform the system sensitivity analysis. Thus, the algorithm provides sensitivity information over the entire design space of interest (global sensitivity), and not only around one operating point (local sensitivity). Although the method [19] is very accurate and more efficient with respect to the perturbative approach, it suffers from a high computational cost when the size of the MNA matrices of the PEEC circuits becomes large. In [21], a parameterized sensitivity analysis based on a parameterized model order reduction (PMOR) technique is presented. The finite element method is used to generate the equations of the original network, a multiparameter moment matching PMOR technique and an adjoint variable method are used to calculate frequency-domain sensitivities.

In this paper, we propose a new parameterized model order reduction (PMOR) technique to efficiently perform global time- and frequency-domain sensitivity analysis of electromagnetic systems over the design space of interest. The PEEC method is adopted to generate a set of PEEC MNA equations and corresponding state-space matrices at a set of design space points. For each of these points in the design space, the block Laguerre-SVD algorithm is proposed to reduce the size of the original equations of the PEEC-based equivalent circuit along with those describing the port voltage and current sensitivities. Then, a methodology based on a multivariate cubic spline interpolation is used to build a parameterized compact model of port voltages and currents along with their corresponding sensitivities over the entire design space of interest. The proposed technique shows a significantly improved efficiency when performing a global sensitivity analysis with respect to the method [19], while maintaining a high accuracy.

The paper is organized as follows. Section II briefly describes the PEEC formulation and the sensitivity formulation while Section III presents the proposed parameterized model order reduction algorithm. Finally some numerical examples are presented in Section IV to validate the proposed technique.

II. PEEC SENSITIVITY FORMULATION

In what follows, we consider a quasi-static PEEC formulation [12]. The Galerkin's approach is applied to convert the continuous electromagnetic problem described by the EFIE to a discrete problem in terms of electrical circuit quantities, i.e., currents $\boldsymbol{i}(t)$ and

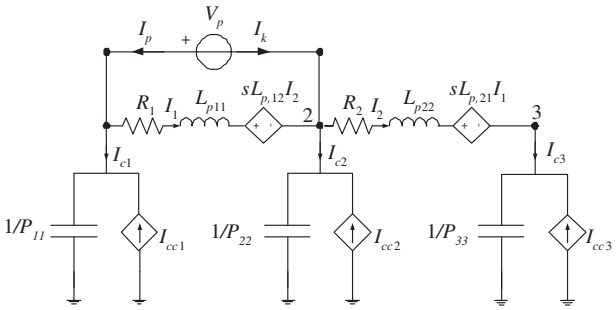

Fig. 1. Illustration of PEEC circuit electrical quantities for a conductor elementary cell.

node potentials $\boldsymbol{v}(t)$. An example of PEEC electrical quantities for a conductor elementary cell is illustrated, in the Laplace domain, in Fig. 1 where the current controlled voltage sources $sL_{p,ij}I_j$ and the current controlled current sources I_{cci} model the magnetic and electric field coupling, respectively. Let us denote with n_n the number of the nodes and with n_b the number of branches where currents flow. Among this latter, n_c and n_d represent the branches of conductors and dielectrics, respectively. Furthermore, let us assume to be interested in generating an admittance ($\mathbf{Y}$) representation having n_p output currents $\boldsymbol{i}_p(t)$ under voltage excitation $\boldsymbol{v}_p(t)$. Using the MNA formulation [17], the following admittance representation is obtained [20]:

$$\begin{bmatrix} \mathbf{P} & \mathbf{0}_{n_n,n_b} & \mathbf{0}_{n_n,n_d} & \mathbf{0}_{n_n,n_p} \\ \mathbf{0}_{n_b,n_n} & \mathbf{L}_p & \mathbf{0}_{n_b,n_d} & \mathbf{0}_{n_b,n_p} \\ \mathbf{0}_{n_d,n_n} & \mathbf{0}_{n_d,n_b} & \mathbf{C}_d & \mathbf{0}_{n_d,n_p} \\ \mathbf{0}_{n_p,n_n} & \mathbf{0}_{n_p,n_b} & \mathbf{0}_{n_p,n_d} & \mathbf{0}_{n_p,n_p} \end{bmatrix} \frac{d}{dt} \begin{bmatrix} \boldsymbol{q}(t) \\ \boldsymbol{i}(t) \\ \boldsymbol{v}_d(t) \\ \boldsymbol{i}_k(t) \end{bmatrix} = - \begin{bmatrix} \mathbf{0}_{n_n,n_n} & -\mathbf{P}\mathbf{A}^{\mathrm{T}} & \mathbf{0}_{n_n,n_d} & \mathbf{P}\mathbf{K}^{\mathrm{T}} \\ \mathbf{A}\mathbf{P} & \mathbf{R} & \mathbf{\Phi} & \mathbf{0}_{n_b,n_p} \\ \mathbf{0}_{n_d,n_n} & -\mathbf{\Phi}^{\mathrm{T}} & \mathbf{0}_{n_d,n_d} & \mathbf{0}_{n_d,n_p} \\ -\mathbf{K}\mathbf{P} & \mathbf{0}_{n_p,n_b} & \mathbf{0}_{n_p,n_d} & \mathbf{0}_{n_p,n_p} \end{bmatrix} \cdot \begin{bmatrix} \boldsymbol{q}(t) \\ \boldsymbol{i}(t) \\ \boldsymbol{v}_d(t) \\ \boldsymbol{i}_k(t) \end{bmatrix} + \begin{bmatrix} \mathbf{0}_{n_n+n_b+n_d,n_p} \\ -\mathbf{I}_{n_p,n_p} \end{bmatrix} \cdot \big[\boldsymbol{v}_p(t)\big], \quad (1)$$

$$\boldsymbol{i}_p(t) = \begin{bmatrix} \mathbf{0}_{n_n+n_b+n_d,n_p} \\ -\mathbf{I}_{n_p,n_p} \end{bmatrix}^T \cdot \begin{bmatrix} \boldsymbol{q}(t) \\ \boldsymbol{i}(t) \\ \boldsymbol{v}_d(t) \\ \boldsymbol{i}_k(t) \end{bmatrix}, \quad (2)$$

where $\mathbf{P} \in \mathbb{R}^{n_n \times n_n}$ and $\mathbf{L}_p \in \mathbb{R}^{n_b \times n_b}$ are the coefficients of potential and partial inductance matrices, respectively, $\mathbf{R} \in \mathbb{R}^{n_b \times n_b}$ is a diagonal matrix containing the resistances of volume cells and $\mathbf{C}_d \in \mathbb{R}^{n_d \times n_d}$ is the excess capacitance matrix describing the polarization charge in dielectrics [22]. $\mathbf{A} \in \mathbb{R}^{n_b \times n_n}$ is the connectivity matrix, while $\mathbf{K} \in \mathbb{R}^{n_p \times n_n}$ is a selection matrix introduced to define the port voltages in terms of node potentials:

$$\boldsymbol{v}_p(t) = \mathbf{K}\ \boldsymbol{v}(t). \quad (3)$$

In (1), $\boldsymbol{q}(t) \in \mathbb{R}^{n_n \times 1}$ represents the charges on the conductors, $\boldsymbol{i}(t) \in \mathbb{R}^{n_b \times 1}$ is the vector of volume currents, $\boldsymbol{v}_d(t) \in \mathbb{R}^{n_d \times 1}$ describes the voltage drop across the excess capacitance and $\boldsymbol{i}_k(t) \in \mathbb{R}^{n_p \times 1}$ represents the port currents. $\mathbf{I}_{n_p,n_p}$ is the identity matrix of dimension equal to the number of ports and $\mathbf{\Phi}$ is:

$$\mathbf{\Phi}=\begin{bmatrix}\mathbf{0}_{n_c,n_d}\\ \mathbf{I}_{n_d,n_d}\end{bmatrix}. \tag{4}$$

The vector $\boldsymbol{i}_p(t)$ describes the n_p port currents that are of opposite sign with respect to $\boldsymbol{i}_k(t)$. The system of equations (1)-(2) is typically ill-conditioned because the values of charges are usually much smaller than those of currents and voltages. In order to mitigate such a problem, a scaling scheme can be adopted [20]. Equations (1)-(2) can be easily translated from the $\mathbf{Y}$ representation to an impedance ($\mathbf{Z}$) representation [19] that can be expressed in a compact form as:

$$\begin{aligned}\mathbf{C}\,\dot{\boldsymbol{x}}(t)&=-\mathbf{G}\,\boldsymbol{x}(t)+\mathbf{B}\,\boldsymbol{i}_p(t)\\ \boldsymbol{v}_p(t)&=\mathbf{L}^{\mathrm{T}}\boldsymbol{x}(t),\end{aligned} \tag{5}$$

where $\mathbf{C} \in \mathbb{R}^{n_s \times n_s}$, $\mathbf{G} \in \mathbb{R}^{n_s \times n_s}$, $\mathbf{B} \in \mathbb{R}^{n_s \times n_p}$, $\mathbf{L} = \mathbf{B}$, $\boldsymbol{x}(t) = [\boldsymbol{q}(t)\ \boldsymbol{i}(t)\ \boldsymbol{v}_d(t)]^{\mathrm{T}} \in \mathbb{R}^{n_s \times 1}$ and $n_s = n_n + n_b + n_d$ is the number of state variables [19].

Considering now the influence of the design parameters $\boldsymbol{g} = (g_1, ..., g_{\mathrm{M}})$, the formulation (5) becomes:

$$\begin{aligned}\mathbf{C}(\boldsymbol{g})\,\dot{\boldsymbol{x}}(t,\boldsymbol{g})&=-\mathbf{G}(\boldsymbol{g})\mathbf{x}(t,\boldsymbol{g})+\mathbf{B}(\boldsymbol{g})\,\boldsymbol{i}_p(t)\\ \boldsymbol{v}_p(t,\boldsymbol{g})&=\mathbf{L}^{T}(\boldsymbol{g})\mathbf{x}(t,\boldsymbol{g}).\end{aligned} \tag{6}$$

In [19], the sensitivity of the voltage outputs with respect to M design parameters $\boldsymbol{g} = (g_m)_{m=1}^{M}$ was computed deriving (6). Merging the original system and corresponding sensitivity system, a new full system can be written as:

$$\begin{aligned}\begin{bmatrix}\mathbf{C}(\boldsymbol{g}) & 0\\ \widehat{\mathbf{C}}(\boldsymbol{g})\mathbf{C}(\boldsymbol{g})\end{bmatrix}\begin{bmatrix}\dot{\boldsymbol{x}}(t,\boldsymbol{g})\\ \dot{\widehat{\boldsymbol{x}}}(t,\boldsymbol{g})\end{bmatrix} &= -\begin{bmatrix}\mathbf{G}(\boldsymbol{g}) & 0\\ \widehat{\mathbf{G}}(\boldsymbol{g})\mathbf{G}(\boldsymbol{g})\end{bmatrix}\begin{bmatrix}\boldsymbol{x}(t,\boldsymbol{g})\\ \widehat{\boldsymbol{x}}(t,\boldsymbol{g})\end{bmatrix}\\ &\quad+\begin{bmatrix}\mathbf{B}(\boldsymbol{g}) & 0\\ \widehat{\mathbf{B}}(\boldsymbol{g})\mathbf{B}(\boldsymbol{g})\end{bmatrix}\begin{bmatrix}\boldsymbol{i}_p(t,\boldsymbol{g})\\ \widehat{\boldsymbol{i}}_p(t,\boldsymbol{g})\end{bmatrix}\\ \begin{bmatrix}\boldsymbol{v}_p(t,\boldsymbol{g})\\ \widehat{\boldsymbol{v}}_p(t,\boldsymbol{g})\end{bmatrix} &= \begin{bmatrix}\mathbf{L}(\boldsymbol{g})\widehat{\mathbf{L}}(\boldsymbol{g})\\ 0\quad\ \mathbf{L}(\boldsymbol{g})\end{bmatrix}^{\mathrm{T}}\begin{bmatrix}\boldsymbol{x}(t,\boldsymbol{g})\\ \widehat{\boldsymbol{x}}(t,\boldsymbol{g})\end{bmatrix},\end{aligned} \tag{7}$$

where $\widehat{\cdot}$ denotes the derivatives with respect to the design parameters. Equation (7) can be solved, applying appropriate termination conditions, by the means of differential equations solvers, upon the knowledge of the system matrices and their derivatives. However, the simulations become slow and difficult to manage when the dimensions of the original PEEC matrices become large. Therefore, it is fundamental to obtain a parameterized reduced order model able to reduce the CPU time effort needed to carry out the desired simulations.

III. PARAMETERIZED MODEL ORDER REDUCTION ALGORITHM

In this section, we describe the proposed PMOR algorithm applied to the system (7) in order to perform parameterized (global) time- and frequency-domain sensitivity analysis with respect to design parameters in a more efficient way in comparison with the technique [19], where a parameterized sensitivity analysis was performed using interpolation models of the original PEEC matrices without any order reduction scheme.

A. Block model order reduction

The first step of the proposed PMOR algorithm is to generate a set of PEEC matrices $\{\mathbf{P}(\boldsymbol{g}_k), \mathbf{L}_p(\boldsymbol{g}_k), \mathbf{C}_d(\boldsymbol{g}_k), \mathbf{R}(\boldsymbol{g}_k)\}_{k=1}^{K_{tot}}$ corresponding to a set of K_{tot} initial samples $\boldsymbol{g}_k$ in the design space. We assume that a topologically fixed discretization mesh is used and that it is independent from the specific design parameter values as in [19]. When geometrical parameters are modified, the mesh is only locally stretched or shrunk. Therefore, the PEEC matrices $\mathbf{A}, \mathbf{\Phi}, \mathbf{K}$ are uniquely determined by the circuit topology and do not depend on $\boldsymbol{g}$. Then, a model order reduction (MOR) is proposed to generate the Krylov matrix $\mathbf{K}_q(\boldsymbol{g}_k)$ of the system (7) for each initial sample in the design space. In [23, 24], block structure preserving MOR methods were presented, where blocks were derived based on the specific application. This concept of block structure preserving MOR is used in this paper to generalize the Laguerre-SVD MOR (LSVD-MOR) algorithm [25]. The standard LSVD-MOR is listed in Algorithm 1, where α is a positive scaling parameter, $q-1$ is the order of approximation and:

$$\mathbf{K}_q = \left[\mathbf{R}^{(0)}, \mathbf{R}^{(1)}, \ldots, \mathbf{R}^{(q-1)}\right], \tag{8}$$

is the Krylov matrix of order $q-1$ [25]. The LSVD-MOR algorithm can be extended to a block LSVD-MOR method, considering the block form of the matrices in (7). If we replace the set of matrices $\{\mathbf{C}, \mathbf{G}, \mathbf{B}, \mathbf{L}\}$ in Algorithm 1 with that block form, the step $k = 0$ of the standard LSVD-MOR algorithm can be re-written as:

$$\begin{bmatrix}\mathbf{G}+\alpha\mathbf{C} & 0\\ \widehat{\mathbf{G}}+\alpha\widehat{\mathbf{C}}\mathbf{G}+\alpha\mathbf{C}\end{bmatrix}\begin{bmatrix}\mathbf{R}_{11}^{(0)}\mathbf{R}_{12}^{(0)}\\ \mathbf{R}_{21}^{(0)}\mathbf{R}_{22}^{(0)}\end{bmatrix} = \begin{bmatrix}\mathbf{B}\,0\\ \widehat{\mathbf{B}}\mathbf{B}\end{bmatrix}. \tag{9}$$

After some manipulation it follows:

$$\begin{aligned}\begin{bmatrix}\mathbf{R}_{11}^{(0)}\mathbf{R}_{12}^{(0)}\\ \mathbf{R}_{21}^{(0)}\mathbf{R}_{22}^{(0)}\end{bmatrix} &= \begin{bmatrix}\mathbf{G}_N^{-1} & 0\\ \widehat{\mathbf{G}}_N^{-1}\mathbf{G}_N^{-1}\end{bmatrix}\begin{bmatrix}\mathbf{B}\,0\\ \widehat{\mathbf{B}}\mathbf{B}\end{bmatrix} =\\ &\begin{bmatrix}\mathbf{G}_N^{-1}\mathbf{B} & 0\\ \widehat{\mathbf{G}}_N^{-1}\mathbf{B}+\mathbf{G}_N^{-1}\widehat{\mathbf{B}}\mathbf{G}_N^{-1}\mathbf{B}\end{bmatrix} = \begin{bmatrix}\mathbf{R}_1^{(0)} & 0\\ \mathbf{R}_2^{(0)}\mathbf{R}_1^{(0)}\end{bmatrix},\end{aligned} \tag{10}$$

where we have defined $\mathbf{G}_N$ and $\widehat{\mathbf{G}}_N$ as

$$\begin{aligned}\mathbf{G}_N&=\mathbf{G}+\alpha\mathbf{C}\\ \widehat{\mathbf{G}}_N&=\widehat{\mathbf{G}}+\alpha\widehat{\mathbf{C}}.\end{aligned} \tag{11}$$

At the step $k=0$, the Krylov matrix $\mathbf{K}_q$ is composed of two components:

$$\begin{cases}\mathbf{R}_1^{(0)}=\mathbf{G}_N^{-1}\mathbf{B}\\ \mathbf{R}_2^{(0)}=\widehat{\mathbf{G}}_N^{-1}\mathbf{B}+\mathbf{G}_N^{-1}\widehat{\mathbf{B}}.\end{cases} \tag{12}$$

The first component is related to the Krylov matrix of the original system (5) for $k=0$, while the second one is the derivative of this first component:

$$\mathbf{R}_2^{(0)}=\widehat{\mathbf{R}}_1^{(0)}. \tag{13}$$

This means that the Krylov matrix of the original system and its derivative are enough to finalize the first step of the block LSVD-MOR algorithm. The other steps for for $k>0$ lead to:

$$\begin{bmatrix}\mathbf{G}+\alpha\mathbf{C} & 0\\ \widehat{\mathbf{G}}+\alpha\widehat{\mathbf{C}}\mathbf{G}+\alpha\mathbf{C}\end{bmatrix}\begin{bmatrix}\mathbf{R}_{11}^{(k)}\mathbf{R}_{12}^{(k)}\\ \mathbf{R}_{21}^{(k)}\mathbf{R}_{22}^{(k)}\end{bmatrix}=\begin{bmatrix}\mathbf{G}-\alpha\mathbf{C} & 0\\ \widehat{\mathbf{G}}-\alpha\widehat{\mathbf{C}}\mathbf{G}-\alpha\mathbf{C}\end{bmatrix}\begin{bmatrix}\mathbf{R}_{11}^{(k-1)}\mathbf{R}_{12}^{(k-1)}\\ \mathbf{R}_{21}^{(k-1)}\mathbf{R}_{22}^{(k-1)}\end{bmatrix}. \tag{14}$$

Likewise, after some manipulations:

$$\begin{bmatrix}\mathbf{R}_{11}^{(k)}\mathbf{R}_{12}^{(k)}\\ \mathbf{R}_{21}^{(k)}\mathbf{R}_{22}^{(k)}\end{bmatrix}=\begin{bmatrix}\mathbf{G}_N^{-1} & 0\\ \widehat{\mathbf{G}}_N^{-1}\mathbf{G}_N^{-1}\end{bmatrix}\begin{bmatrix}\mathbf{G}_R & 0\\ \widehat{\mathbf{G}}_R\mathbf{G}_R\end{bmatrix}\begin{bmatrix}\mathbf{R}_{11}^{(k-1)}\mathbf{R}_{12}^{(k-1)}\\ \mathbf{R}_{21}^{(k-1)}\mathbf{R}_{22}^{(k-1)}\end{bmatrix}=\begin{bmatrix}\mathbf{G}_N^{-1}\mathbf{G}_R & 0\\ \widehat{\mathbf{G}}_N^{-1}\mathbf{G}_R+\mathbf{G}_N^{-1}\widehat{\mathbf{G}}_R\mathbf{G}_N^{-1}\mathbf{G}_R\end{bmatrix}\begin{bmatrix}\mathbf{R}_1^{(k-1)} & 0\\ \mathbf{R}_2^{(k-1)}\mathbf{R}_1^{(k-1)}\end{bmatrix}, \tag{15}$$

where we have defined $\mathbf{G}_R$ and $\widehat{\mathbf{G}}_R$ as:

$$\begin{aligned}\mathbf{G}_R&=\mathbf{G}-\alpha\mathbf{C}\\ \widehat{\mathbf{G}}_R&=\widehat{\mathbf{G}}-\alpha\widehat{\mathbf{C}}.\end{aligned} \tag{16}$$

The blocks of the Krylov matrix for $k>0$ are also composed of two components:

$$\begin{cases}\mathbf{R}_1^{(k)}=\mathbf{G}_N^{-1}\mathbf{G}_R\mathbf{R}_1^{(k-1)}\\ \mathbf{R}_2^{(k)}=\mathbf{G}_N^{-1}\mathbf{G}_R\mathbf{R}_2^{(k-1)}+\\ \qquad\underbrace{\left(\widehat{\mathbf{G}}_N^{-1}\mathbf{G}_R+\mathbf{G}_N^{-1}\widehat{\mathbf{G}}_R\right)}_{\widehat{\mathbf{G}_N^{-1}\mathbf{G}_R}}\mathbf{R}_1^{(k-1)}.\end{cases} \tag{17}$$

As previously, equation (17) shows that the first component $\mathbf{R}_1^{(k)}$ is the component of the Krylov matrix of the original system (5) for $k>0$, and the second component $\mathbf{R}_2^{(k)}$ is the corresponding derivative:

$$\mathbf{R}_2^{(k)}=\widehat{\mathbf{R}}_1^{(k)}. \tag{18}$$

According to Algorithm 1, the Krylov matrix $\mathbf{K}_q$ reads:

$$\mathbf{K}_q=\left[\begin{array}{c|c|c|c|c|c|c|c}\mathbf{R}_1^{(0)} & 0 & \mathbf{R}_1^{(1)} & 0 & \dots & \mathbf{R}_1^{(q-1)} & 0\\ \mathbf{R}_2^{(0)} & \mathbf{R}_1^{(0)} & \mathbf{R}_2^{(1)} & \mathbf{R}_1^{(1)} & \dots & \mathbf{R}_2^{(q-1)} & \mathbf{R}_1^{(q-1)}\end{array}\right], \tag{19}$$

and by a column permutation:

$$\mathbf{K}_q=\left[\begin{array}{c|c|c|c|c|c|c}\mathbf{R}_1^{(0)} & \dots & \mathbf{R}_1^{(q-1)} & 0 & \dots & 0\\ \mathbf{R}_2^{(0)} & \dots & \mathbf{R}_2^{(q-1)} & \mathbf{R}_1^{(0)} & \dots & \mathbf{R}_1^{(q-1)}\end{array}\right], \tag{20}$$

where $\mathbf{R}_1^{(i)}=\mathbf{R}^{(i)}$ is the i-th component of the Krylov matrix of the original system and $\mathbf{R}_2^{(i)}=\widehat{\mathbf{R}}^{(i)}$ is its derivative (see (13) and (18)). For each initial sample $\boldsymbol{g}_k$ the corresponding Krylov matrix $\mathbf{K}_q(\boldsymbol{g}_k)$ is computed using the block LSVD-MOR method.

To compute the reduced system of (7), an orthonormalization step is applied to the Krylov matrix $\mathbf{K}_q$ using a Singular Value Decomposition (SVD) algorithm to obtain the projection matrix:

$$\mathbf{V}\rightarrow\mathbf{V}\,\Sigma\,\mathbf{U}^{\mathrm{T}}=\mathrm{SVD}\left(\mathbf{K}_q\right), \tag{21}$$

that is then used for the congruence transformations to compute the reduced matrices. In order to preserve the block structure of the system (7), the projection matrix $\mathbf{V}\in\mathbb{R}^{2n_s\times n_r}$ is partitioned in a block fashion [23, 24]:

$$\mathbf{V}=\begin{bmatrix}\mathbf{V}_1\\ \mathbf{V}_2\end{bmatrix}, \tag{22}$$

where $n_r=q\cdot n_p$ denotes the column size of the Krylov matrix $\mathbf{K}_q$. The projection matrix blocks may not have a full column rank n_r, in particular the first block $\mathbf{V}_1$, due to the presence of a block of zeros. An orthonormalization step is applied to $\mathbf{V}_1$ in order to obtain a matrix $\widetilde{\mathbf{V}}_1$ whose columns span the same space as the columns of $\mathbf{V}_1$, while having however a full column rank [24]. The same operation is performed on $\mathbf{V}_2$ to obtain $\widetilde{\mathbf{V}}_2$. The second block $\mathbf{V}_2$ has generally full column rank n_r. After this step the column size of the two blocks $\widetilde{\mathbf{V}}_1$ and $\widetilde{\mathbf{V}}_2$ may differ with respect to the column size of $\mathbf{V}_1$ and $\mathbf{V}_2$. However, this does not influence the reduction of the full system (7). Finally the projection matrix is written as [23, 24]:

$$\widetilde{\mathbf{V}}=\begin{bmatrix}\widetilde{\mathbf{V}}_1 & 0\\ 0 & \widetilde{\mathbf{V}}_2\end{bmatrix}. \tag{23}$$

In order to reduce the overall system in (7), the projection matrix (23) is used to compute the reduced matrices by congruence transformations:

$$\begin{aligned}\begin{bmatrix}\mathbf{C}_{r,1} & 0\\ \widehat{\mathbf{C}}_{r,2}\mathbf{C}_{r,2}\end{bmatrix}&=\begin{bmatrix}\widetilde{\mathbf{V}}_1^{\mathrm{T}} & 0\\ 0 & \widetilde{\mathbf{V}}_2^{\mathrm{T}}\end{bmatrix}\begin{bmatrix}\mathbf{C} & 0\\ \widehat{\mathbf{C}}\mathbf{C}\end{bmatrix}\begin{bmatrix}\widetilde{\mathbf{V}}_1 & 0\\ 0 & \widetilde{\mathbf{V}}_2\end{bmatrix}\\ \begin{bmatrix}\mathbf{G}_{r,1} & 0\\ \widehat{\mathbf{G}}_{r,2}\mathbf{G}_{r,2}\end{bmatrix}&=\begin{bmatrix}\widetilde{\mathbf{V}}_1^{\mathrm{T}} & 0\\ 0 & \widetilde{\mathbf{V}}_2^{\mathrm{T}}\end{bmatrix}\begin{bmatrix}\mathbf{G} & 0\\ \widehat{\mathbf{G}}\mathbf{G}\end{bmatrix}\begin{bmatrix}\widetilde{\mathbf{V}}_1 & 0\\ 0 & \widetilde{\mathbf{V}}_2\end{bmatrix}\\ \begin{bmatrix}\mathbf{B}_{r,1} & 0\\ \widehat{\mathbf{B}}_{r,2}\mathbf{B}_{r,2}\end{bmatrix}&=\begin{bmatrix}\widetilde{\mathbf{V}}_1^{\mathrm{T}} & 0\\ 0 & \widetilde{\mathbf{V}}_2^{\mathrm{T}}\end{bmatrix}\begin{bmatrix}\mathbf{B} & 0\\ \widehat{\mathbf{B}}\mathbf{B}\end{bmatrix}\\ \begin{bmatrix}\mathbf{L}_{r,1}\widehat{\mathbf{L}}_{r,2} & \\ 0 & \mathbf{L}_{r,2}\end{bmatrix}&=\begin{bmatrix}\widetilde{\mathbf{V}}_1^{\mathrm{T}} & 0\\ 0 & \widetilde{\mathbf{V}}_2^{\mathrm{T}}\end{bmatrix}\begin{bmatrix}\mathbf{L}\widehat{\mathbf{L}} & \\ 0 & \mathbf{L}\end{bmatrix}.\end{aligned} \tag{24}$$

Algorithm 2 lists the steps of the proposed block LSVD-MOR method to perform in order to obtain

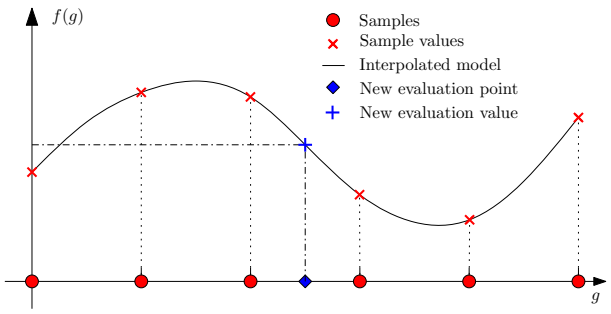

Fig. 2. Example of sampling design space grid.

the set of reduced matrices for the reduced system. Concerning the proposed PMOR algorithm, the block LSVD-MOR method is used to to generate the Krylov matrix $\mathbf{K}_q(\boldsymbol{g}_k)$ of the system (7) for each initial sample in the design space.

B. Interpolation models

Once the set of matrices $\{\mathbf{P}(\boldsymbol{g}_k), \mathbf{L}_p(\boldsymbol{g}_k), \mathbf{C}_d(\boldsymbol{g}_k), \mathbf{R}(\boldsymbol{g}_k), \mathbf{K}_q(\boldsymbol{g}_k)\}_{k=1}^{K_{tot}}$ is available, the corresponding interpolation models are built. Figure 2 shows an example for the case of one design parameter. Each interpolation model is built starting from a set of samples indicated with red dots ($\circ$) in Fig. 2. For each ($\circ$) sample in the design space, a set of PEEC matrices and a Krylov matrix are computed and the corresponding models, that cover the entire design space, are built by the means of an interpolation scheme. For interpolation purposes the multivariate cubic spline interpolation method [26], which is well-known for its stable and smooth characteristics, is used. The proposed interpolation scheme is continuous in the first and second order derivatives and can be used in the general case of an M-dimensional (M-D) design space.

First, the interpolation models $\left\{\overline{\mathbf{P}}(\boldsymbol{g}), \overline{\mathbf{L}}_p(\boldsymbol{g}), \overline{\mathbf{C}}_d(\boldsymbol{g}), \overline{\mathbf{R}}(\boldsymbol{g})\right\}$ are computed while guaranteeing positive definiteness and semidefiniteness matrix properties [19, 20]. At this step, according to Algorithm 2, it could be possible to compute a set of reduced matrices for each point of interest in the design space by using the block LSVD-MOR method previously described. However, to improve the efficiency of the proposed PMOR method, we choose to create an interpolation model for the $\mathbf{K}_q(\boldsymbol{g})$ matrix, starting from the corresponding data samples $\mathbf{K}_q(\boldsymbol{g}_k)$. From the model $\overline{\mathbf{K}}_q(\boldsymbol{g})$, the values of the projection matrices $\mathbf{V}_1(\boldsymbol{g})$ and $\mathbf{V}_2(\boldsymbol{g})$ can be computed for each point of interest in the design space.

Inspecting equation (19), only the interpolation models of the matrices $\{\mathbf{R}_1^{(i)}(\boldsymbol{g}_k)\}_{i=0}^{q-1}$ and $\{\mathbf{R}_2^{(i)}(\boldsymbol{g}_k)\}_{i=0}^{q-1}$ (namely $\{\overline{\mathbf{R}}_1^{(i)}(\boldsymbol{g})\}_{i=0}^{q-1}$ and $\{\overline{\mathbf{R}}_2^{(i)}(\boldsymbol{g})\}_{i=0}^{q-1}$) are sufficient to obtain the interpolation model $\overline{\mathbf{K}}_q(\boldsymbol{g})$. Furthermore, there is still one degree of freedom about how to compute the matrices $\{\mathbf{R}_2^{(i)}(\boldsymbol{g})\}_{i=0}^{q-1}$:

1. As described in Algorithm 2;
2. directly as derivative of $\{\overline{\mathbf{R}}_1^{(i)}(\boldsymbol{g})\}_{i=0}^{q-1}$ (see (13) and (18)).

The latter option is based on the interpolation model $\{\overline{\mathbf{R}}_1^{(i)}(\boldsymbol{g})\}_{i=0}^{q-1}$ that can provide derivatives with respect to $\boldsymbol{g}$. This choice is preferred since it allows storing only the model $\{\overline{\mathbf{R}}_1^{(i)}(\boldsymbol{g})\}_{i=0}^{q-1}$ and then saving memory resources, while keeping a similar accuracy.

Using the interpolation models $\left\{\overline{\mathbf{P}}(\boldsymbol{g}), \overline{\mathbf{L}}_p(\boldsymbol{g}), \overline{\mathbf{C}}_d(\boldsymbol{g}), \overline{\mathbf{R}}(\boldsymbol{g})\right\}$ and $\{\overline{\mathbf{R}}_1^{(i)}(\boldsymbol{g})\}_{i=0}^{q-1}$, it is possible to obtain a set of PEEC matrices and a set of projection matrices $\mathbf{V}_1(\boldsymbol{g})$ and $\mathbf{V}_2(\boldsymbol{g})$ for each point of the design space. Applying the congruence transformations, the sets of reduced matrices $\{\mathbf{C}_{r,i}(\boldsymbol{g}), \mathbf{G}_{r,i}(\boldsymbol{g}), \mathbf{B}_{r,i}(\boldsymbol{g}), \mathbf{L}_{r,i}(\boldsymbol{g})\}_{i=1,2}$ and $\left\{\widehat{\mathbf{C}}_{r,2}(\boldsymbol{g}), \widehat{\mathbf{G}}_{r,2}(\boldsymbol{g}), \widehat{\mathbf{B}}_{r,2}(\boldsymbol{g}), \widehat{\mathbf{L}}_{r,2}(\boldsymbol{g})\right\}$ are computed. The reduced version of (7) can be written as:

$$\begin{aligned}
&\begin{bmatrix} \mathbf{C}_{r,1}(\boldsymbol{g}) & 0 \\ \widehat{\mathbf{C}}_{r,2}(\boldsymbol{g})\mathbf{C}_{r,2}(\boldsymbol{g}) & \end{bmatrix} \begin{bmatrix} \dot{\boldsymbol{x}}_r(t,\boldsymbol{g}) \\ \dot{\widehat{\boldsymbol{x}}}_r(t,\boldsymbol{g}) \end{bmatrix} = \\
&- \begin{bmatrix} \mathbf{G}_{r,1}(\boldsymbol{g}) & 0 \\ \widehat{\mathbf{G}}_{r,2}(\boldsymbol{g})\mathbf{G}_{r,2}(\boldsymbol{g}) & \end{bmatrix} \begin{bmatrix} \boldsymbol{x}_r(t,\boldsymbol{g}) \\ \widehat{\boldsymbol{x}}_r(t,\boldsymbol{g}) \end{bmatrix} \\
&+ \begin{bmatrix} \mathbf{B}_{r,1}(\boldsymbol{g}) & 0 \\ \widehat{\mathbf{B}}_{r,2}(\boldsymbol{g})\mathbf{B}_{r,2}(\boldsymbol{g}) & \end{bmatrix} \begin{bmatrix} \boldsymbol{i}_p(t,\boldsymbol{g}) \\ \widehat{\boldsymbol{i}}_p(t,\boldsymbol{g}) \end{bmatrix} \\
&\begin{bmatrix} \boldsymbol{v}_p(t,\boldsymbol{g}) \\ \widehat{\boldsymbol{v}}_p(t,\boldsymbol{g}) \end{bmatrix} = \begin{bmatrix} \mathbf{L}_{r,1}(\boldsymbol{g})\widehat{\mathbf{L}}_{r,2}(\boldsymbol{g}) \\ 0 \quad \mathbf{L}_{r,2}(\boldsymbol{g}) \end{bmatrix}^{\mathrm{T}} \begin{bmatrix} \boldsymbol{x}_r(t,\boldsymbol{g}) \\ \widehat{\boldsymbol{x}}_r(t,\boldsymbol{g}) \end{bmatrix}. \qquad (25)
\end{aligned}$$

These reduced matrices are used to perform both time- and frequency-domain sensitivity analysis, with appropriate termination conditions.

IV. NUMERICAL EXAMPLES

Two numerical examples are proposed to validate the proposed PMOR technique for sensitivity analysis. Parameterized time- and frequency-domain sensitivity analyses are performed with the proposed PMOR technique and the results are compared with the approach proposed in [19] and with the perturbative approach (with respect to each parameter g_m) that in time- and frequency-domain reads:

$$\widehat{\boldsymbol{v}}_{p,g_m}(t,\boldsymbol{g}) = \frac{\boldsymbol{v}_p(t,g_1,..,g_m+\Delta g_m,..,g_M) - \boldsymbol{v}_p(t,\boldsymbol{g})}{\Delta g_m}, \qquad (26)$$

$$\widehat{\mathbf{Z}}_{g_m}(s,\boldsymbol{g}) = \frac{\mathbf{Z}(s,g_1,..,g_m+\Delta g_m,..,g_M) - \mathbf{Z}(s,\boldsymbol{g})}{\Delta g_m}, \qquad (27)$$

where $m = 1, \ldots, M$, M and Δg_m represent the number of parameters and the increment, respectively. The accuracy of the perturbative approach depends on the choice of the increment Δg_m: if the increment is not small enough, the estimation of the derivative is not accurate, while if the perturbation is very small compared with the nominal value, numerical problems may occur due to numerical noise. This may lead to inaccurate computation of the system sensitivities. In contrast, thanks to the interpolation models, the methods presented in this paper and in [19] lead to more accuracy and numerical stability, since the derivatives are computed from continuously differentiable polynomials built by means of spline functions. The method [19] is denoted as Full Parameterized while the proposed method is denoted as Block PMOR in what follows.

In the numerical results (see Tables 1-2), for the Full Parameterized and Block PMOR models, the model evaluation CPU time indicates the average time needed to evaluate the corresponding parameterized models in a point of the validation grid in order to obtain a set of PEEC matrices. Moreover, for the Block PMOR model, the SVD operation is also part of the model evaluation. For the Perturbative Approach, the model evaluation CPU time refers to the average time needed to compute a set of PEEC matrices by a PEEC solver at and around a point in the validation grid, which are then used for a finite difference calculation. Once the parameterized models are evaluated, or PEEC matrices have been computed (perturbative approach), they can be used to carry out sensitivity analysis in frequency- and time-domain. For each of the three methods, the average time needed to perform the sensitivity analysis in a point of the validation grid is denoted as simulation CPU time.

Numerical simulations have been performed on a Linux platform on an AMD FX(tm)-6100 Six-Core Processor 3.3 GHz with 16 GB RAM.

A. Metallic enclosure coupled to a transmission line

In the first example a metallic enclosure coupled to a transmission line is studied. The cross section is shown in Fig. 3. The geometrical dimensions are $w_c = 1\,\text{mm}$, $d_c = 5\,\text{mm}$, $s_l = 1\,\text{mm}$, $d_l = 30\,\text{mm}$. A set of PEEC matrices is computed over a grid of 6×6 values of the conductor length $l_c \in [25 - 65]$ mm and $s_c \in [7 - 22]$ mm in order to build the aforementioned parameterized reduced order model. Furthermore, a parameterized full model has been built by means of the method [19] for the comparison. The order of the full models is 2870 while the reduced order is 471. Parameterized time- and frequency-domain sensitivities are performed over a validation grid of 5×5 values of $l_c \in [29 - 61]$ mm and $s_c \in [8.5 - 20.5]$ mm. The obtained results are then compared with the ones obtained by the perturbative model (26), (27). For the time-domain results, the bottom conductor is excited by a smooth pulse voltage source with amplitude 1V, rise/fall times $\tau_r = \tau_f = 1.5$ ns, width 6 ns and internal resistance $R_T = 50\ \Omega$. All the ports are terminated on 50 Ω resistances.

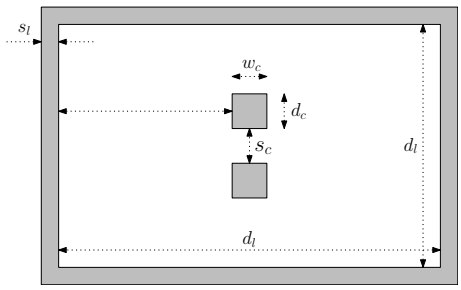

Fig. 3. Metallic enclosure coupled to a transmission line (example A).

Table 1: Simulation time comparison (Example A). The CPU time information related to time- and frequency-domain analysis refers to an average value of the CPU time needed to perform the sensitivity analysis in a point of the validation grid

		Block PMOR	Full Parameterized	Perturbative Approach
Time	*Model eval*	13 s	12 s	618 s
	Simulation	6 s	161 s	48 s
	Total	19 s	173 s	666 s
Freq	*Model eval*	13 s	12 s	618 s
	Simulation	37 s	639 s	944 s
	Total	50 s	651 s	1562 s

Figures 4-5 and 6-7 show time- and frequency-domain results that confirm the high accuracy of the proposed approach. Table 1 clearly shows the computational advantage of the proposed PMOR technique: the CPU time required to perform both time- and frequency-domain sensitivity simulations is considerably improved with respect to the two other compared approaches for a sensitivity analysis around a nominal design point and therefore also for a global sensitivity analysis. It is important to note that the Block PMOR and Full Parameterized methods require a one-time effort to build the corresponding parameterized models that then allow global sensitivity simulations. This CPU time for the Block PMOR method is equal to 8236 s and for the Full Parameterized method is equal to 7513 s.

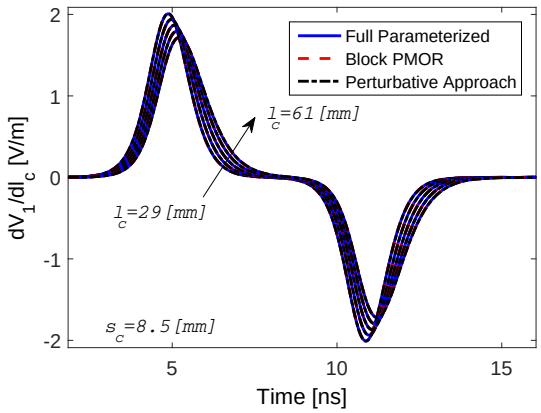

Fig. 4. Time-domain voltage sensitivity with respect to l_c at the port 1 (example A).

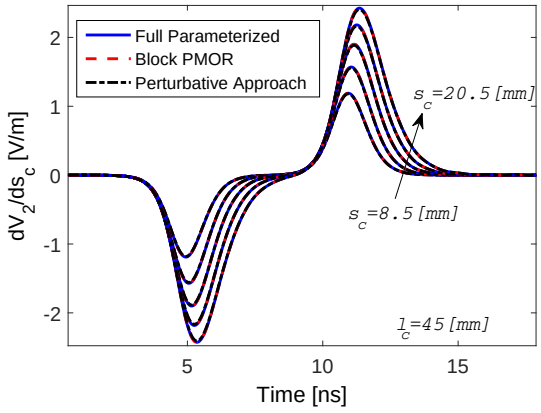

Fig. 5. Time-domain voltage sensitivity with respect to s_c at the port 2 (example A).

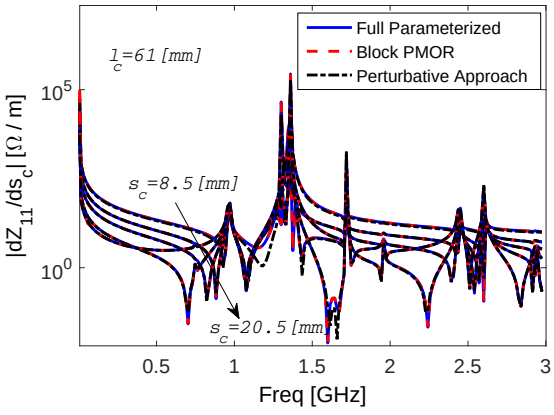

Fig. 6. Magnitude of the sensitivity of Z_{11} with respect to s_c (example A).

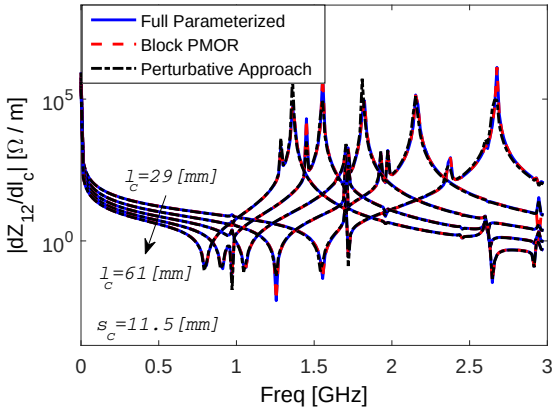

Fig. 7. Magnitude of the sensitivity of Z_{12} with respect to l_c (example A).

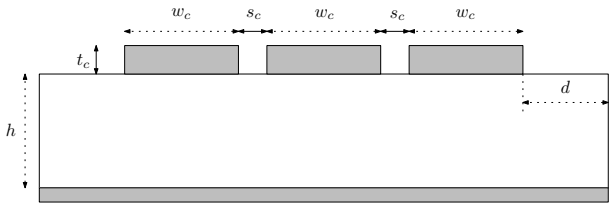

Fig. 8. Three conductors microstrip (example B).

B. Three conductors microstrip

Three coupled microstrips are modeled in this example and Fig. 8 shows the corresponding cross section. The geometrical dimensions are $w_c = 178\,\mu$m, $t_c = 35\,\mu$m, $d = 3$ mm and the length of the lines is $l = 40$ mm. The parameterized reduced order and parameterized full models have been built starting from a set of PEEC matrices computed over a grid of 6×6 values of $s_c \in [0.1 - 0.4]$ mm and $h \in [0.1 - 0.3]$ mm. The order of the full models is 3360 while the reduced order is 577. Parameterized time- and frequency-domain sensitivities are performed over a validation grid of 5×5 values of $s_c \in [0.13 - 0.37]$ mm and $h \in [0.12 - 0.28]$ mm. The obtained results are then compared with the perturbative approach (26), (27). For the time-domain results, a smooth pulse voltage source with amplitude 1V, rise/fall times $\tau_r = \tau_f = 1.5$ ns, width 6 ns and internal resistance $R_T = 50\ \Omega$ is applied on the first conductor. All the ports are terminated on 50 Ω resistances. Time-domain sensitivity results are shown in Figs. 9, 10 while frequency-domain sensitivity results are shown in Figs. 11, 12. As in the previous example, the results confirm the high accuracy of the proposed method. Table 2 shows the simulation time comparison that clearly confirms that the proposed PMOR method considerably reduces the CPU time

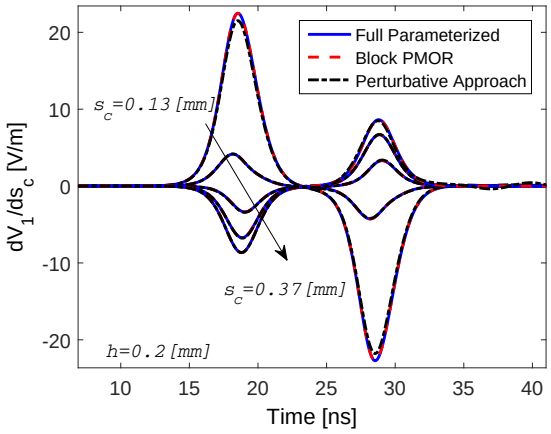

Fig. 9. Time-domain voltage sensitivity with respect to s_c at the port 1 (example B).

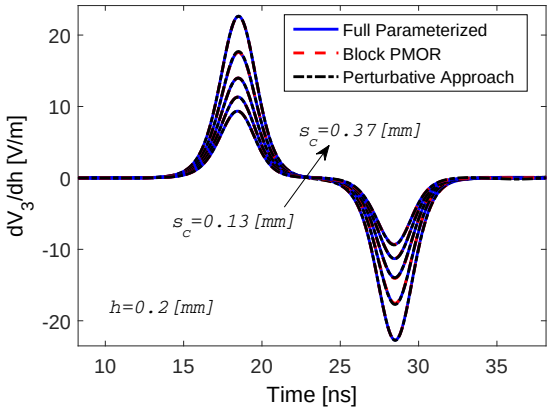

Fig. 10. Time-domain voltage sensitivity with respect to h at the port 3 (example B).

required for a sensitivity analysis with respect to the other two methods around a nominal design point and therefore for a global sensitivity analysis. As in the previous example, an initial computational effort is required to compute the Block PMOR and Full Parameterized models that is equal to 9306 s for the Block PMOR and to 8456 s for the Full Parameterized method.

V. CONCLUSIONS

In this paper we have presented a new PMOR technique to perform both time- and frequency-domain global sensitivity analysis of PEEC circuits. It is based on the PEEC method, the block Laguerre SVD model order reduction technique and interpolation schemes. Two numerical examples confirm the high modeling capability and the improved efficiency of the proposed approach with respect to existing sensitivity analysis methods.

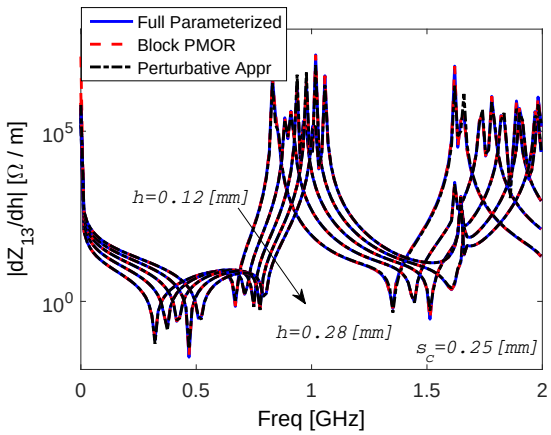

Fig. 11. Magnitude of the sensitivity of Z_{13} with respect to h (example B).

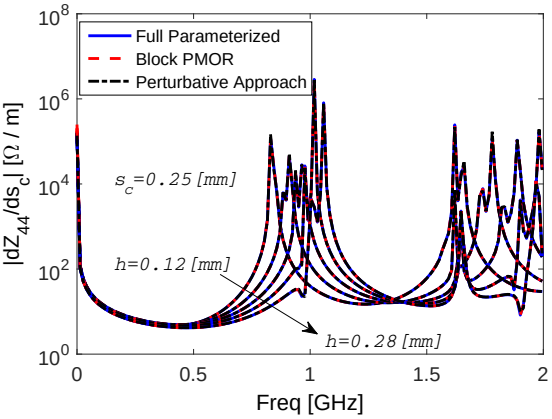

Fig. 12. Magnitude of the sensitivity of Z_{44} with respect to s_c (example B).

Table 2: Simulation time comparison (Example B). The CPU time information related to time- and frequency-domain analysis refers to an average value of the CPU time needed to perform the sensitivity analysis in a point of the validation grid

		Block PMOR	Full Parameterized	Perturbative Approach
Time	*Model eval*	11 s	10 s	699 s
	Simulation	9 s	275 s	48 s
	Total	20 s	285 s	747 s
Freq	*Model eval*	11 s	10 s	699 s
	Simulation	52 s	591 s	857 s
	Total	63 s	601 s	1556 s

VI. APPENDIX

This appendix illustrates the pseudo-code of the Laguerre-SVD and the Block Laguerre-SVD algorithms.

Algorithm 1 Laguerre-SVD Algorithm

Select values for α and q
$\mathbf{R}^{(0)} \leftarrow (\mathbf{G}+\alpha\mathbf{C})\,\mathbf{R}^{(0)} = \mathbf{B}$
for $k = 1 \rightarrow q-1$ **do**
  $\mathbf{R}^{(k)} \leftarrow (\mathbf{G}+\alpha\mathbf{C})\,\mathbf{R}^{(k)} = (\mathbf{G}-\alpha\mathbf{C})\,\mathbf{R}^{(k-1)}$
end for
$\mathbf{K}_q = \left[\mathbf{R}^{(0)}, \mathbf{R}^{(1)}, \ldots, \mathbf{R}^{(q-1)}\right]$
$\mathbf{V}\Sigma\mathbf{U}^{\mathrm{T}} \leftarrow \mathrm{SVD}\,[\mathbf{K}_q]$
$\mathbf{C}_r \leftarrow \mathbf{V}^{\mathrm{T}}\mathbf{C}\mathbf{V}, \quad \mathbf{G}_r \leftarrow \mathbf{V}^{\mathrm{T}}\mathbf{G}\mathbf{V}$
$\mathbf{B}_r \leftarrow \mathbf{V}^{\mathrm{T}}\mathbf{B}, \quad \mathbf{L}_r \leftarrow \mathbf{V}^{\mathrm{T}}\mathbf{L}$

Algorithm 2 Block Laguerre-SVD Algorithm

Select values for α and q
$\mathbf{G}_N \leftarrow \mathbf{G}+\alpha\mathbf{C}, \quad \mathbf{G}_R \leftarrow \mathbf{G}-\alpha\mathbf{C}$
$\widehat{\mathbf{G}}_N \leftarrow \widehat{\mathbf{G}}+\alpha\widehat{\mathbf{C}}, \quad \widehat{\mathbf{G}}_R \leftarrow \widehat{\mathbf{G}}-\alpha\widehat{\mathbf{C}}$
$\mathbf{R}_1^{(0)} \leftarrow \mathbf{G}_N^{-1}\mathbf{B}$
$\mathbf{R}_2^{(0)} \leftarrow \widehat{\mathbf{G}}_N^{-1}\mathbf{B} + \mathbf{G}_N^{-1}\widehat{\mathbf{B}}$
for $k = 1 \rightarrow q-1$ **do**
  $\mathbf{R}_1^{(k)} \leftarrow \mathbf{G}_N^{-1}\mathbf{G}_R\mathbf{R}_1^{(k-1)}$
  $\mathbf{R}_2^{(k)} \leftarrow \left(\widehat{\mathbf{G}}_N^{-1}\mathbf{G}_R + \mathbf{G}_N^{-1}\widehat{\mathbf{G}}_R\right)\mathbf{R}_1^{(k-1)} + \mathbf{G}_N^{-1}\mathbf{G}_R\mathbf{R}_2^{(k-1)}$
end for
$\mathbf{K}_q = \left[\begin{array}{ccc|ccc} \mathbf{R}_1^{(0)} & \ldots & \mathbf{R}_1^{(q-1)} & 0 & \ldots & 0 \\ \mathbf{R}_2^{(0)} & \ldots & \mathbf{R}_2^{(q-1)} & \mathbf{R}_1^{(0)} & \ldots & \mathbf{R}_1^{(q-1)} \end{array}\right]$
$n_r = q \cdot n_p$
$\mathbf{V} \leftarrow \mathbf{V}\,\Sigma\,\mathbf{U}^{\mathrm{T}} = \mathrm{SVD}\,(\mathbf{K}_q)$
$\mathbf{V} = \begin{bmatrix}\mathbf{V}_1 \\ \mathbf{V}_2\end{bmatrix}$

for $i = 1, 2$ **do**
  If rank $\mathbf{V}_i = r_{V_i} < n_r$ determine an $n_s \times r_{V_i}$ matrix $\widetilde{\mathbf{V}}_i$ with colspan $\widetilde{\mathbf{V}}_i$ = colspan $\mathbf{V}_i$ and rank $\widetilde{\mathbf{V}}_i = r_{Vi}$
end for
$\widetilde{\mathbf{V}} = \begin{bmatrix}\widetilde{\mathbf{V}}_1 & 0 \\ 0 & \widetilde{\mathbf{V}}_2\end{bmatrix}$
Apply congruence transformations (24)

ACKNOWLEDGMENT

This work was supported by the Research Foundation Flanders (FWO-Vlaanderen). Ferranti is currently a Post-Doctoral Research Fellow of FWO-Vlaanderen.

REFERENCES

[1] J. P. Webb, "Design sensitivity of frequency response in 3-D finite-element analysis of microwave devices," *IEEE Transactions on Magnetics*, vol. 35, pp. 1109–1112, Mar. 2002.

[2] S. Ali, N. N. Nikolova, and M. H. Bakr, "Sensitivity analysis with full-wave electromagnetic solvers based on structured grids," *IEEE Transactions on Magnetics*, vol. 40, no. 3, pp. 1521–1530, May 2004.

[3] N. K. Nikolova and M. H. Bakr, "An adjoint variable method for time-domain transmission-line modeling with fixed structured grids," *IEEE Transactions on Microwave Theory and Techniques*, vol. 52, no. 2, pp. 554–559, Feb. 2004.

[4] E. A. Soliman, M. H. Bakr, and N. K. Nikolova, "An adjoint variable method for sensitivity calculations of multiport devices," *IEEE Transactions on Microwave Theory and Techniques*, vol. 52, no. 2, Feb. 2004.

[5] N. K. Nikolova, J. W. Bandler, and M. H. Bakr, "Adjoint techniques for sensitivity analysis in high frequency structure CAD," *IEEE Transactions on Microwave Theory and Techniques*, vol. 52, no. 1, pp. 403–419, Jan. 2004.

[6] Y. Yang, T. Hallerod, D. Ericsson, A. Hellervik, A. Bondeson, and T. Rylander, "Gradient optimization of microwave devices using continuum design sensitivities from the adjoint problem," *IEEE Transactions on Magnetics*, vol. 41, no. 5, pp. 1780–1783, May 2005.

[7] N. K. Nikolova, J. Zhu, D. Li, M. H. Bakr, and J. W. Bandler, "Sensitivity analysis of network parameters with electromagnetic frequency-domain simulators," *IEEE Transactions on Microwave Theory and Techniques*, vol. 54, no. 2, pp. 670–681, Feb. 2006.

[8] N. Nikolova, X. Zhu, Y. Song, A. Hasib, and M. Bakrare, "S-Parameter sensitivities for electromagnetic optimization based on volume field solutions," *IEEE Transactions on Microwave Theory and Techniques*, vol. 57, no. 6, pp. 1526–1538, Jun. 2009.

[9] N. Nikolova, H. Tam, and M. Bakr, "Sensitivity analysis with the FDTD method on structured grids," *IEEE Transactions on Microwave Theory and Techniques*, vol. 52, no. 4, pp. 1207–1216, Apr. 2004.

[10] P. Basl, M. Bakr, and N. Nikolova, "Efficient estimation of sensitivities in TLM with dielectric discontinuities," *IEEE Microwave and Wireless Components Letters*, vol. 15, no. 2, pp. 89–91, Feb. 2005.

[11] A. E. Ruehli and P. A. Brennan, "Efficient capacitance calculations for three-dimensional multiconductor systems," *IEEE Transactions on Microwave Theory and Techniques*, vol. 21, no. 2, pp. 76–82, Feb. 1973.

[12] A. E. Ruehli, "Equivalent circuit models for three dimensional multiconductor systems," *IEEE Transactions on Microwave Theory and Techniques*, vol. MTT-22, no. 3, pp. 216–221, Mar. 1974.

[13] K. Coperich, A. Ruehli, and A. Cangellaris, "Enhanced skin effect for partial-element equivalent circuit (PEEC) models," *IEEE Transactions on Microwave Theory and Techniques*, vol. 48, no. 9, pp. 1435–1442, Sep. 2000.

[14] B. Archembeault and A. Ruehli, "Analysis of power/ground-plane EMI decoupling performance using the partial-element equivalent circuit technique," *IEEE Transactions on Electromagnetic Compatibility*, vol. 43, no. 4, pp. 437–445, Nov. 2001.

[15] P. J. Restle, A. Ruehli, S. G. Walker, and G. Papadopoulos, "Full-wave PEEC time-domain for the modeling of on-chip interconnects," *IEEE Transactions on Computer-Aided Design*, vol. 20, no. 7, pp. 877–887, Jul. 2001.

[16] G. Antonini, D. Deschrijver, and T. Dhaene, "Broadband macromodels for retarded Partial Element Equivalent Circuit (rPEEC) method," *IEEE Transactions on Electromagnetic Compatibility*, vol. 49, no. 1, pp. 34–48, Feb. 2007.

[17] C. Ho, A. Ruehli, and P. Brennan, "The modified nodal approach to network analysis," *IEEE Transactions on Circuits and Systems*, pp. 504–509, Jun. 1975.

[18] C. A. Balanis, *Advanced Engineering Electromagnetics*, John Wiley and Sons, New York, 1989.

[19] L. De Camillis, F. Ferranti, G. Antonini, D. Vande Ginste, and D. De Zutter, "Parameterized partial element equivalent circuit method for sensitivity analysis of multiport systems," *IEEE Transactions on Components, Packaging and Manufacturing Technology*, vol. 2, no. 2, pp. 248–255, Feb. 2012.

[20] F. Ferranti, G. Antonini, T. Dhaene, L. Knockaert, and A. Ruehli, "Physics-based passivity-preserving parameterized model order reduction for PEEC circuit analysis," *IEEE Transactions on Components, Packaging and Manufacturing Technology*, vol. 1, no. 3, pp. 399–409, Mar. 2011.

[21] M. Ahmadloo and A. Dounavis, "Sensitivity analysis of microwave circuits using parameterized model order reduction techniques," *IEEE Transactions on Components, Packaging and Manufacturing Technology*, vol. 1, no. 11, pp. 1795–1805, Nov. 2011.

[22] A. E. Ruehli and H. Heeb, "Circuit models for three-dimensional geometries including dielectrics," *IEEE Transactions on Microwave Theory and Techniques*, vol. 40, no. 7, pp. 1507–1516, Jul. 1992.

[23] H. Yu, L. He, and S. Tar, "Block structure preserving model order reduction," in *Behavioral Modeling and Simulation Workshop, 2005. BMAS 2005. Proceedings of the 2005 IEEE International*, pp. 1–6, Sep. 2005.

[24] R. W. Freund, "The SPRIM algorithm for structure-preserving order reduction of general RCL circuits," *Model Reduction for Circuit Simulation. Lecture Notes in Electrical Engineering*, vol. 74, pp. 25–52, 2011.

[25] L. Knockaert and D. De Zutter, "Laguerre-SVD reduced-order modeling," *IEEE Transactions on Microwave Theory and Techniques*, vol. 48, no. 9, pp. 1469–1475, Sep. 2000.

[26] C. De Boor, *A Practical Guide to Splines*, Springer-Verlag Berlin and Heidelberg GmbH & Co. K, 1978.

Luca De Camillis received the B.S. and M.S. degrees in Computer Science Engineering from Università degli Studi dell'Aquila, L'Aquila, Italy, in 2005 and 2007, respectively. He collaborated with the Electromagnetics Group, Department of Information Technology, Ghent University, Ghent, with the Department of Electrical Engineering, Università degli Studi dell'Aquila and with the ACE Laboratory, University of Washington, Seattle. His current research interests include parametric macromodeling and sensitivity analysis.

Giulio Antonini received the Laurea degree (*cum laude*) in Electrical Engineering from University of L'Aquila, L'Aquila, Italy, in 1994 and the Ph.D. degree in Electrical Engineering from University of Rome "La Sapienza" in 1998. Since 1998, he has been with the UAq EMC Laboratory, University of L'Aquila, where he is currently a Professor. His scientific interests are in the field of computational electromagnetics.

Francesco Ferranti received the B.S. degree in Electronic Engineering from the Università degli Studi di Palermo, Palermo, Italy, in 2005, the M.S. degree in Electronic Engineering from the Università degli Studi dell'Aquila, L'Aquila, Italy, in 2007, and the Ph.D. degree in Electrical Engineering from Ghent University, Ghent, Belgium, in 2011. He is currently an Assistant Professor at the Department of Fundamental Electricity and Instrumentation, Vrije Universiteit Brussel, Brussels, Belgium. His research interests include parameterized macromodeling and model order reduction, applied electromagnetics, behavioral modeling, adaptive sampling, system identification, microwave design and characterization, electro-thermal modeling, uncertainty quantification and optimization.